Desalination and Water Treatment
www.deswater.com

doi: 10.5004/dwt.2023.29845

304 (2023) 228–237
August

Adsorption performance of antibiotics using magnetized–nitrated semi-carbonized fiber loaded with metal ions

Wen-bin Li[a,†], Jiang-ming Ou-yang[a,†], Ke Xie[b,†], Hong-yan Deng[a,*], Yin-fei Wang[a,*], Touqeer Abbas[c], Bixia Wang[a]

[a]*College of Environmental Science and Engineering, China West Normal University, Nanchong Sichuan 637009, China, emails: lwb062@163.com (W.-b. Li), 1442682026@qq.com (J.-m. Ou-yang), dhongyan119@163.com (H.-y. Deng), wyinfei820@163.com (Y.-f. Wang), wangbixia@cwnu.edu.cn (B.-x. Wang)*
[b]*Sichuan Chuanqian Expressway Co., Ltd., Gulin 646500, China, email: paper_l@163.com (K. Xie)*
[c]*Department of Soil, Water, and Climate, University of Minnesota, Twin 637009, USA, email: abbastouqeer@yahoo.com (A. Touqeer)*

Received 24 May 2023; Accepted 10 August 2023

ABSTRACT

This study investigated the adsorption performance of antibiotics using modified semi-carbonized fibers (SCF) prepared from polyacrylonitrile and loaded with metal ions. Nitrated semi-carbonized fibers (N-SCF) and magnetized–nitrated semi-carbonized fibers (MN-SCF) were prepared through nitrification and magnetization methods, and different metal ion-loaded MN-SCFs were obtained by loading Ca and Mg ions onto MN-SCF. The effects of pH, temperature, and ionic strength on antibiotic adsorption were analyzed. The adsorption kinetics and thermodynamics of tetracycline (TC), chlortetracycline (CTC), and oxytetracycline (OTC) were studied using batch experiments. Results showed that (1) the adsorption of antibiotics on the tested materials initially increased and then decreased with increasing pH and ionic strength, reaching maximum values at pH 4 and 0.1 mol/L, respectively. (2) Higher temperatures facilitated the adsorption of antibiotics on the materials, which followed a chemisorption mechanism. (3) The Langmuir model provided a better fit for the adsorption isotherms of TC, CTC, and OTC compared with the Freundlich model, suggesting monolayer adsorption. (4) The maximum adsorption capacity (q_m) of the antibiotics ranged from 0.80 to 3.97 mg/g, with of CTC > OTC > TC. Metal ion-loaded MN-SCFs exhibited higher adsorption amounts compared with MN-SCF alone.

Keywords: Semi-carbonized fiber; Magnetized–nitrated treatment; Ion loading; Antibiotic; Adsorption amount

1. Introduction

The increasing global concern over the occurrence of antibiotics as emerging organic contaminants in the environment, coupled with heightened awareness of environmental security and advancements in modern analysis technologies, has prompted extensive research in this field [1,2]. Antibiotics are extensively used for treating infectious diseases, resulting in a substantial dosage of antibiotics used annually in the aquaculture industry, estimated to be approximately 10 million tons, including chemically synthesized antibiotics and veterinary drugs [3,4]. However, a substantial portion of these antibiotics, approximately 30%–90%, is excreted as parent compounds or metabolites through urine or faeces [5]. If left untreated, then the residual antibiotics in the environment can pose substantial risks to ecological systems and human health [6]. Therefore, efficient removal of antibiotic pollution and restoration of contaminated soil and water environments are crucial research priorities.

* Corresponding authors.
† These authors have contributed equally to this work and share first authorship.

In recent years, material adsorption has emerged as a promising approach for pollution remediation research due to its cost-effectiveness, simplicity, and proven efficacy [7,8]. Carbon fiber materials, known for their large specific surface area and cation exchange capacity, have been widely employed for remediating soil and water environments contaminated with antibiotics [9]. For instance, Zhang et al. [10] demonstrated that activated carbon fiber (ACF) efficiently removes sulfadiazine from water, offering a low-cost, energy-efficient, and easily scalable adsorbent with industrial potential. Hydrochloric acid modification of ACF improved its ability to remove heavy metal ions and antibiotics from water, achieving removal rates above 90% for Zn(II), Cr(VI), and sulfamethoxazole (SMX) [11]. Liu et al. [12] reported excellent catalytic performance of phosphorus-doped carbon fibers in SMX removal, with a removal rate exceeding 90% and a mineralization rate of 82.75%. Moreover, magnetized and nitrated treatments of carbon materials have been shown to enhance their pollutant adsorption capacity. Li [13] observed substantial improvement in the adsorption capacity of carbon materials for Cu(II) through nitrification reduction modification, outperforming similar activated carbon materials. Under identical experimental conditions, the modified carbon material exhibited approximately fourfold capacity compared with the original material. Zhang et al. prepared magnetized carbon materials and observed enhanced adsorption capacity for phenanthrene after magnetization [14]. In addition, magnetic biochar demonstrated effective adsorption of Pb(II) in water due to its magnetic separation capability when magnetized through the precipitation method [15].

To further enhance the adsorption capacity of carbon fiber materials, researchers have explored the incorporation of metal ions to introduce additional surface-active sites and enhance their physical and chemical properties [16]. Chen et al. [17] found that the addition of metal oxides during biochar preparation substantially improved its adsorption capacity for various pollutants, and magnesium-modified biochar showed excellent efficacy in nitrogen and phosphorus treatment in water [18]. Loading Fe, Mn, and Mg ions onto biochar substantially increased its specific area and pore volume, thereby enhancing its adsorption capacity [19]. These findings collectively indicate that loading metal ions, magnetized treatment all contribute to improving the adsorption capacity of carbon fiber materials for pollutants. If metal ions are loaded onto the material after magnetized and nitrated modification, then the adsorption capacity of the composite-modified material for pollutants is expected to be improved. However, research on the combination of magnetized-nitrated treatment and metal ion loading of carbon fiber materials for the pollutant adsorption is lacking.

In this study, semi-carbonized fiber (SCF) was prepared using polyacrylonitrile and modified to produce nitrated semi-carbonized fibers (N-SCF) and magnetized–nitrated semi-carbonized fibers (MN-SCF). Different metal ion-loaded MN-SCFs were obtained by loading Ca and Mg ions on the surface of MN-SCF. The effects of environmental factors, such as pH, temperature, and ionic strength on the adsorption of antibiotics onto the tested materials were analyzed. The kinetic and thermodynamic characteristics of the adsorption process of tetracycline (TC), chlortetracycline (CTC), and oxytetracycline (OTC) were studied using the batch method. The results provide valuable insights for the development of composite carbon fiber materials and the optimization of their adsorption properties.

2. Materials and method

2.1. Experimental materials

Polyacrylonitrile fiber, obtained from Langfang City, Hebei Province, was used as the raw material. Metal salt solutions, including $MgCl_2$ and $CaCl_2$, $CaCO_3$, and $Ca(OH)_2$, were purchased from Chengdu Cologne Chemical Co., Ltd., (Chengdu, China). TC, CTC, and OTC with purities exceeding 99% were sourced from Shanghai Aladdin Biochemical Technology Co., Ltd., (Shanghai, China).

2.1.1. Preparation of SCF

Polyacrylonitrile was ground and passed through a 40-mesh sieve. The ground material was then soaked in deionized water for 24 h and subsequently decolorized using ethanol. After decolorization, the raw material was placed in a muffle furnace at 300°C and stored in an anaerobic environment for 2 h. Following cooling, the material was ground through a 60-mesh screen to obtain SCF.

2.1.2. Preparation of MN-SCF

A certain amount of SCF was selected and placed into a 250 mL stopped-triangle flask. A specific volume of 34% HNO_3 solution (based on the SCF volume) was added to the flask. The flask was then corked and placed in a constant temperature oscillator for 8 h at 25°C [20]. After shaking, the mixture of SCF and nitric acid was filtered using medium-speed filter paper. The N-SCF obtained was subsequently washed repeatedly with deionized water until the filtrate reached a neutral pH of 7. This N-SCF was labelled N-SCF. MN-SCF was then prepared using the coprecipitation supported Fe_3O_4 method [21].

2.1.3. Preparation of calcium and magnesium ion-loaded MN-SCF

A specific amount of MN-SCF was weighed and added to prepared solutions of $MgCl_2$. The mass ratio of metal ions to MN-SCF set to 0.2, with a solid–liquid ratio of 1:10 and a temperature of 25°C. The sample was subjected to ultrasonic oscillation at 100 Hz for 2 h, followed by centrifugation (4,000 rpm) for 15 min. The separated Mg-loaded MN-SCF (Mg-MN-SCF) was repeatedly washed with dH_2O, cooled to room temperature, and ground through a 100-mesh sieve [22,23]. The same method was applied to load $CaCl_2$, $CaCO_3$ and $Ca(OH)_2$ onto Mg-MN-SCF. This resulted in three types of metal ion-loaded MN-SCF, and labelled $CaCl_2$/Mg-MN-SCF, $CaCO_3$/Mg-MN-SCF, and $Ca(OH)_2$/Mg-MN-SCF.

2.2. Experimental design

2.2.1. Influence of experimental factors

The initial pH values of the solution were set as 2, 4, 6, 8, and 10; the solution temperature was set as 35°C; and the

ionic strength was set as 0.1 mol/L NaCl. The experimental temperatures were set at 25°C, 35°C, and 45°C; the pH of the solution was set at 6; and the ionic strength was set at 0.1 mol/L NaCl. The initial ionic strength of the solution was set to 0.05, 0.1, and 0.5 mol/L NaCl; the solution temperature was set to 35°C; and the pH value was set to 6.

2.2.2. Kinetics adsorption of antibiotics

The adsorption time was set as 5, 10, 30, 60, 120, 180, 240, 300, 360, 480, 720, and 1,440 min. The temperature was set as 35°C, the pH value of the solution was set as 6, and the ionic strength was set as 0.1 mol/L NaCl.

2.2.3. Adsorption isotherms of antibiotics

The concentrations of TC, CTC and OTC were set at nine concentration gradients of 0.3, 0.6, 1.2, 3, 6, 12, 18, 24, and 30 mg/L [24]. The temperature was set at 35°C, the pH value of the solution was set as 6, and the ionic strength was set as 0.1 mol/L NaCl.

2.2.4. Morphology properties of the tested materials

The morphology properties of the SCF, MN-SCF, and $Ca(OH)_2$/Mg-MN-SCF were characterized by Fourier-transform infrared spectroscopy (FTIR), scanning electron microscopy (SEM) and energy-dispersive X-ray spectroscopy (EDS).

2.3. Experimental methods

Batch equilibrium method was used for antibiotic adsorption. A total of 0.2000 g of the sample was weighed in nine 50 mL plastic centrifuge tubes and added with 20 mL of antibiotic solutions with different concentration gradients. The samples were oscillated at 25°C and 200 rpm for 12 h at constant temperature [25] and centrifuged at 4,800 rpm for 10 min. The concentration of antibiotics in the supernatant was determined, and the equilibrium adsorption amount was calculated by subtraction method. All the above measurements were inserted into standard solution for analytical quality control.

FTIR analysis was performed on the Nicolet iS50 Type Fourier-transform infrared spectrometer (Thermo Fisher, Massachusetts, USA). SEM-EDS was performed using the Japanese Hitachi S-4800 scanning electron microscope.

2.4. Data processing

2.4.1. Calculation of equilibrium adsorption capacity

The equilibrium adsorption capacity can be calculated according to Eq. (1):

$$q = \frac{\left(C_0 - C_e\right)V}{m} \tag{1}$$

where V is the volume of solution (mL); c_0 is the antibiotic concentration at the starting point (mg/L); c_e is the antibiotic concentration at the equilibrium point (mg/L); m is the mass of tested sample (g); and q is the equilibrium adsorption capacity of tested sample for antibiotics (mg/g).

2.4.2. Fitting of adsorption isotherms

The Langmuir and Freundlich model [26] was selected to fit the adsorption isotherms of the three antibiotics according to the adsorption isotherm trend. Eqs. (2)–(3) are expressed as follows:

$$q = \frac{q_m bc}{1 + bc} \tag{2}$$

$$q = kC_e^{1/n} \tag{3}$$

where q is the equilibrium adsorption amount of antibiotics for the amended soil, mg/g; c is the equilibrium concentration of antibiotics in the solution, mg/L; q_m is the maximum adsorption amount of antibiotics for the tested sample, mg/g; b and n are the apparent equilibrium constant of antibiotic adsorption on the tested sample for the measurement of adsorption affinity. k is a parameter related to the adsorption capacity.

2.4.3. Fitting of adsorption kinetics model

The pseudo-first-order and pseudo-second-order kinetics equation models were used to simulate the adsorption process of three antibiotics on different modified materials [27,28]. The kinetics equations were defined as Eqs. (4)–(5):

$$\ln\left(q_e - q_t\right) = \ln q_e - k_1 t \tag{4}$$

$$\frac{t}{q_t} = \frac{1}{q_e^2 k_2} + \frac{t}{q_e} \tag{5}$$

where q_t is the adsorption capacity corresponding to the adsorbent at time t (mg/g); q_e is the equilibrium adsorption capacity of tested sample for antibiotics (mg/g); k_1 and k_2 are pseudo-first-order and pseudo-second-order reaction rate constants respectively; t is the adsorption time (min).

CurveExpert 1.4 fitting software was used in isothermal fitting, and Origin 9.0 was adopted to improve data plotting. SPSS 16.0 statistical analysis software was used to process the experimental data for variance and correlation analysis.

3. Results and discussion

3.1. Effect of pH and ionic strength on antibiotic adsorption

The adsorption amounts of TC, CTC, and OTC by the tested materials exhibited an initial increased followed by a decrease as the pH increased within the range of pH 2–10 (Fig. 1). The maximum adsorption was observed at pH 4. Beyond pH 4, the adsorption of antibiotics decreased, with a decrease range of 27.54%–70.67% for TC, 29.43%–63.90% for CTC, and 32.61%–66.10% for OTC. The molecular structures of the antibiotics contained three ionizable groups, and their ionization equilibrium constants pK_{a1}, pK_{a2}, and

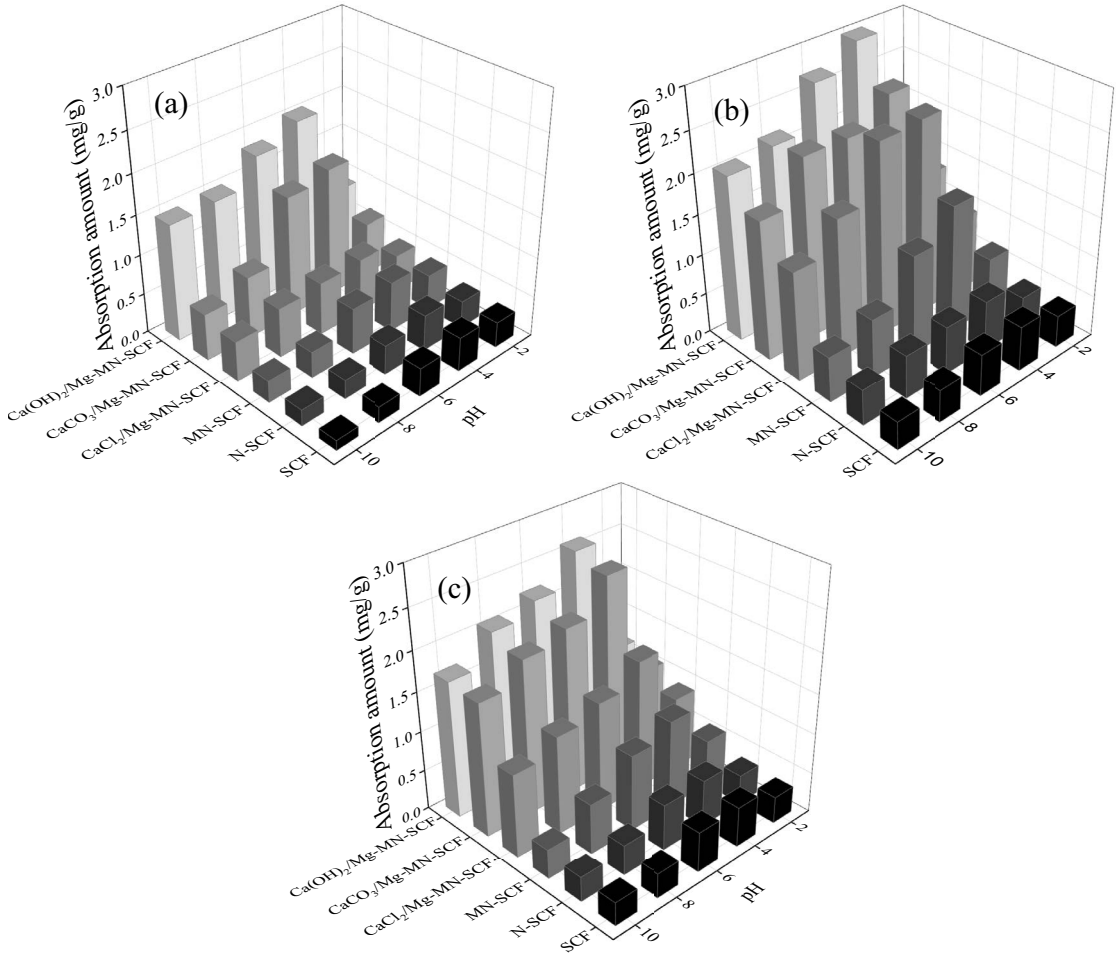

Fig. 1. Effect of pH on the adsorption of TC (a), CTC (b), and OTC (c).

pK_{a3} were determined as 3.30–3.57, 7.49–7.69, and 9.44–9.88, respectively. Antibiotics are positively charged at pH values below 3.30, can exist as positively or negatively charged species between pH 3.30 and 7.69, and are predominantly in anionic form at pH above 9.50 [29]. Under acidic conditions, cation exchange occurs between the antibiotics and the negative charges on the surface of the tested materials, leading to increased adsorption. As the pH increases beyond the optimal value 4, the proportion of negative charges in the antibiotic molecule increases, resulting in a gradual decrease in adsorption.

Fig. 2 depicts the effect of ionic strength on the adsorption of TC, CTC and OTC by the tested materials. The adsorption amounts of all three antibiotics exhibited an increasing trend followed by a decrease as the ionic strength increased from 0.05 to 0.5 mol/L, with the peak adsorption observed at an ionic strength of 0.1 mol/L. When the ionic strength changed from 0.05 to 0.1 mol/L, the adsorption amounts of TC, CTC, and OTC increased by 12.85%–42.71% (TC), 3.34%–47.17% (CTC), and 3.50%–68.01% (OTC), respectively. This observation can be attributed to the influence of ionic strength on the hydrophobic properties of antibiotic molecules. Low Na^+ concentration in the solution enhances the solubility of antibiotics. However, as the Na^+ concentration increases, it competes with antibiotics for adsorption sites on the sample surface, thereby hindering the adsorption of antibiotics by the tested materials [30].

3.2. Effect of temperature on antibiotic adsorption

The influence of temperature on the adsorption of TC, CTC and OTC by different SCF materials is shown in Fig. 3. As the temperature increased from 25°C to 45°C, the adsorption amount of antibiotics by the tested material increased, indicating a positive temperature effect [31]. The adsorption amounts of TC, CTC, and OTC by the SCF materials increased by 48.92%–122.35%, 15.82%–75.43% and 12.53%–79.94%, respectively. The increased temperature enhanced the binding of antibiotic molecules in the solution, leading to increased contact between the antibiotics and the material surface [32]. Therefore, the adsorption capacity of the tested materials increased with the increase of temperature.

3.3. Adsorption kinetic characteristics of antibiotics

The adsorption kinetics curves of TC, CTC and OTC on different SCF materials are shown in Fig. 4. CTC and OTC reached adsorption equilibrium at approximately 120 min,

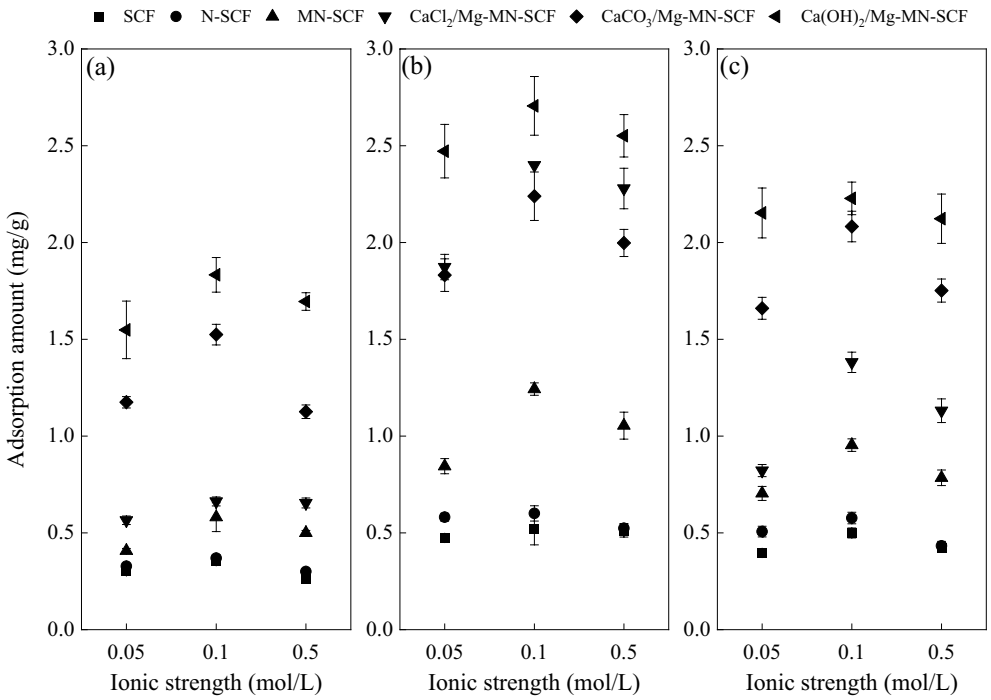

Fig. 2. Effect of ionic strength (I) on the adsorption of TC (a), CTC (b), and OTC (c).

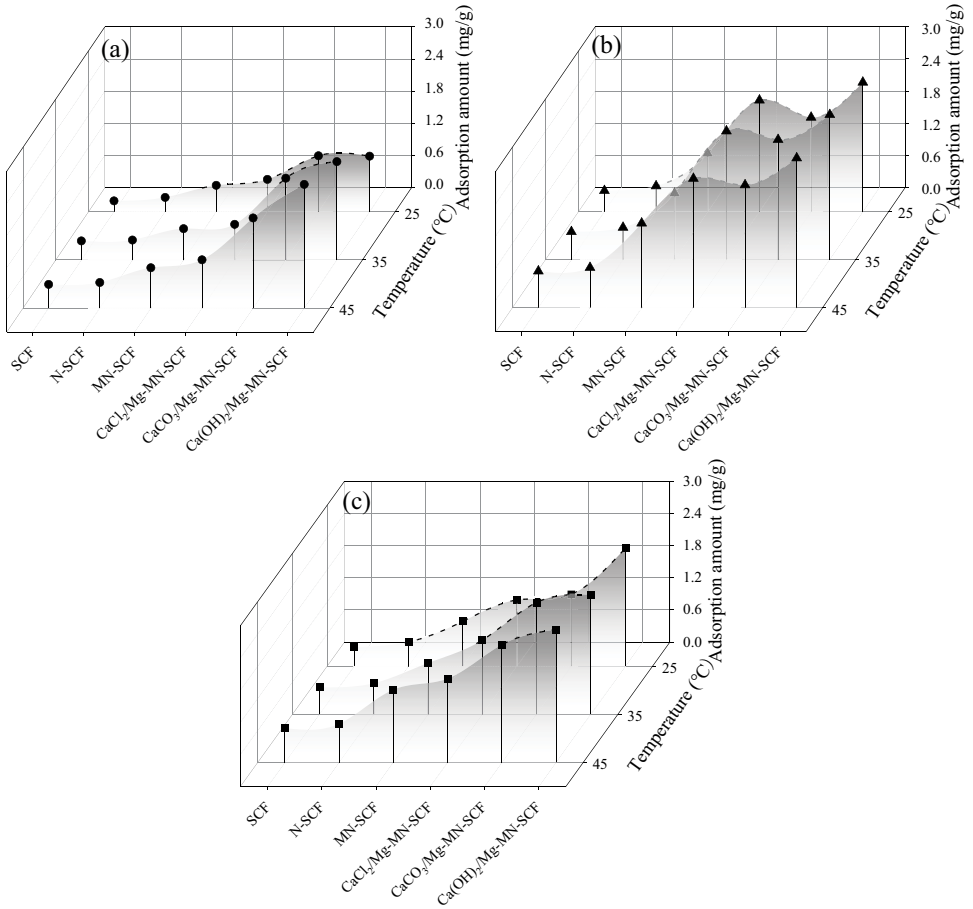

Fig. 3. Effect of temperature on the adsorption of TC (a), CTC (b), and OTC (c).

and TC reached adsorption equilibrium at 180 min. The adsorption process of antibiotics on the tested materials was simulated using pseudo-first-order and pseudo-second-order kinetic equation models. The fitting parameters of the adsorption kinetics are shown in Table 1. The adsorption kinetics of all antibiotics conformed to the pseudo-second-order kinetic equation. The R^2 values of pseudo-second-order kinetic equation for antibiotics adsorption were higher than that of pseudo-first-order kinetic equation. Therefore, the pseudo-second-order kinetic equation model accurately described the adsorption kinetics. The results showed that the adsorption of antibiotics by the tested materials was primarily driven by chemisorption, consistent with the observed temperature effect.

3.4. Adsorption isotherms of antibiotics by different tested materials

The adsorption isotherms of TC, CTC, and OTC on SCF materials under the conditions of 35°C, pH = 6, and ionic strength of 0.1 mol/L, are shown in Fig. 5. The adsorption capacity of TC, OTC, and CTC on the tested materials increased with increasing equilibrium concentration, showing an "L" type pattern. The adsorption isotherms were fitted using the Langmuir and Freundlich models of TC, CTC, and OTC (Table 2). The correlation coefficients for both models reached a high level of significance (P = 0.01). The fitting performance of the Langmuir model was superior to that of the Freundlich model. These results indicated

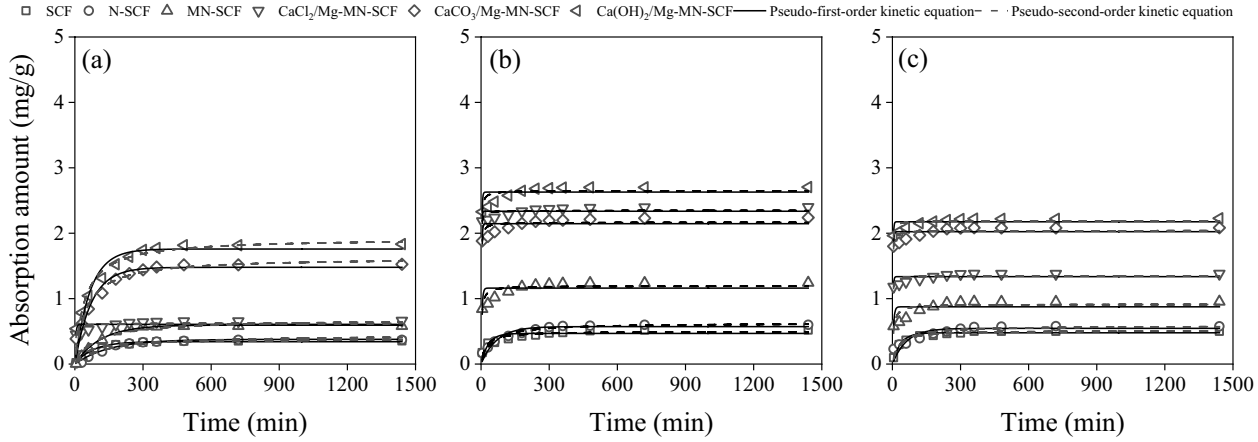

Fig. 4. Adsorption kinetics of TC (a), CTC (b), and OTC (c) on different tested materials.

Table 1
Fitting parameters of adsorption kinetics for TC, CTC, and OTC

Treatments		Pseudo-first-order kinetic equation			Pseudo-second-order kinetic equation		
		q_e (mg/g)	k_1 (min^{-1})	R^2	q_e (mg/g)	k_2 (g/mg·min)	R^2
TC	SCF	0.34	0.0127	0.9771	0.38	0.0466	0.9913
	N-SCF	0.38	0.0066	0.9783	0.45	0.0166	0.9464
	MN-SCF	0.60	0.0089	0.9913	0.68	0.0162	0.9552
	$CaCl_2$/Mg-MN-SCF	0.61	0.2713	0.3220	0.62	0.6156	0.5566
	$CaCO_3$/Mg-MN-SCF	1.48	0.0138	0.9194	1.63	0.0128	0.9506
	$Ca(OH)_2$/Mg-MN-SCF	1.76	0.0150	0.8685	1.92	0.0122	0.9240
CTC	SCF	0.47	0.0319	0.6906	0.50	0.1054	0.8685
	N-SCF	0.57	0.0146	0.8701	0.63	0.0359	0.9315
	MN-SCF	1.16	0.2564	0.3969	1.19	0.2980	0.6415
	$CaCl_2$/Mg-MN-SCF	2.34	0.5451	0.2540	2.35	0.9487	0.4274
	$CaCO_3$/Mg-MN-SCF	2.15	0.4189	0.3667	2.17	0.5147	0.5618
	$Ca(OH)_2$/Mg-MN-SCF	2.63	0.4332	0.3857	2.65	0.4606	0.5820
OTC	SCF	0.48	0.0286	0.9502	0.51	0.0858	0.9931
	N-SCF	0.55	0.0162	0.6161	0.58	0.0504	0.7576
	MN-SCF	0.87	0.2111	0.3371	0.91	0.2344	0.6108
	$CaCl_2$/Mg-MN-SCF	1.34	0.4324	0.3394	1.35	0.8907	0.5293
	$CaCO_3$/Mg-MN-SCF	2.02	0.4412	0.3551	2.04	0.6225	0.5471
	$Ca(OH)_2$/Mg-MN-SCF	2.18	0.4668	0.4343	2.19	0.6917	0.6256

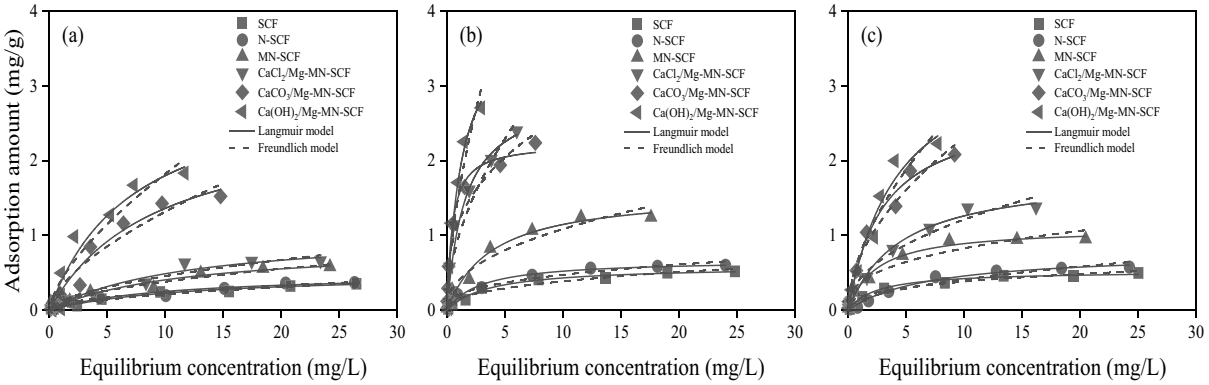

Fig. 5. Adsorption isotherms of TC (a), CTC (b), and OTC (c).

Table 2
Fitting parameters of TC, CTC, and OTC adsorption by the Langmuir and Freundlich model

Samples		Langmuir model				Freundlich model			
		q_m (mg/g)	S	b	r	k	S	n	r
TC	SCF	0.50	0.06	0.08	0.9749**	0.06	0.01	1.79	0.9667**
	N-SCF	0.50	0.10	0.10	0.9092**	0.08	0.01	2.11	0.9607**
	MN-SCF	0.87	0.18	0.09	0.932**	0.11	0.03	1.86	0.9393**
	$CaCl_2$/Mg-MN-SCF	1.06	0.20	0.09	0.9511**	0.12	0.03	1.77	0.9336**
	$CaCO_3$/Mg-MN-SCF	2.62	0.54	0.11	0.9559**	0.31	0.07	1.60	0.9265**
	$Ca(OH)_2$/Mg-MN-SCF	3.11	0.88	0.14	0.9112**	0.40	0.11	1.51	0.8732**
CTC	SCF	0.59	0.03	0.27	0.9845**	0.15	0.02	2.50	0.9412**
	N-SCF	0.67	0.03	0.34	0.9838**	0.21	0.02	2.74	0.9637**
	MN-SCF	1.59	0.11	0.26	0.9817**	0.40	0.06	2.28	0.9460**
	$CaCl_2$/Mg-MN-SCF	2.96	0.44	0.64	0.9264**	0.98	0.14	1.89	0.8906**
	$CaCO_3$/Mg-MN-SCF	2.24	0.08	2.18	0.9892**	1.18	0.10	2.91	0.9356**
	$Ca(OH)_2$/Mg-MN-SCF	3.97	0.63	0.81	0.9507**	1.55	0.15	1.67	0.8939**
OTC	SCF	0.53	0.04	0.41	0.9555**	0.18	0.02	2.93	0.9538**
	N-SCF	0.78	0.06	0.14	0.9829**	0.13	0.03	1.99	0.9267**
	MN-SCF	1.11	0.05	0.42	0.9847**	0.36	0.05	2.80	0.9394**
	$CaCl_2$/Mg-MN-SCF	1.83	0.13	0.22	0.9863**	0.41	0.05	2.14	0.9696**
	$CaCO_3$/Mg-MN-SCF	2.73	0.23	0.34	0.9843**	0.69	0.07	1.91	0.9705**
	$Ca(OH)_2$/Mg-MN-SCF	3.64	0.67	0.23	0.9618**	0.75	0.11	1.74	0.9414**

Note: ** indicates significance at $P = 0.01$ level ($r = 0.765$ at $P = 0.01$ when the degree of freedom $f = 8$);
r is the correlation coefficient
S is the standard error.

that the adsorption of antibiotics on SCF materials primarily occurred through monolayer adsorption [33]. The q_m values of antibiotics on SCF materials ranged from 0.50 to 3.97 mg/g, following the order: $Ca(OH)_2$/Mg-MN-SCF > $CaCl_2$/Mg-MN-SCF and $CaCO_3$/Mg-MN-SCF > MN-SCF > N-SCF > SCF. Among the tested materials, the adsorption capacity exhibited the trend TC < OTC < CTC. The adsorption amounts of MN-SCF and N-SCF for antibiotics increased compared with SCF. Furthermore, the adsorption capacity of ion-loaded MN-SCF for antibiotics was further improved after loading with metal ions, with $Ca(OH)_2$/Mg-MN-SCF exhibiting the highest adsorption effect. The adsorption affinity parameter (k) of the Freundlich model followed the same trend as the q_m values of the Langmuir model. The adsorption intensity (n) of the Freundlich model was higher than the constant (b) in the Langmuir model for antibiotic adsorption. This result can be attributed to the larger specific surface area of $Ca(OH)_2$/Mg-MN-SCF, promoting ion exchange between antibiotics and SCF materials, and facilitating the fixation of antibiotics [34].

3.5. SEM characteristics of the test materials

The SEM images of the different tested materials are shown in Fig. 6a–c. The original SCF exhibited a smooth surface and compact structure. However, the surface of MN-SCF

became rough and fluffy, with the appearance of fine pore structures after magnetized–nitrated treatment. A large number of pore structures and organic phases were observed on the surface of $Ca(OH)_2$/Mg-MN-SCF. The modifier played a crucial role in the modification process, influencing the surface morphology of the modified SCF. The presence of abundant pores in $Ca(OH)_2$/Mg-MN-SCF ensures accessibility for adsorption molecules and provides numerous adsorption sites [35].

3.6. FTIR and EDS analysis of the test materials

Fig. 7a–d shows the FTIR and EDS characteristic peaks of the different SCF materials. The characteristic peaks corresponding to oxygen functional groups include the C=O stretching vibration peak at 1,052 cm^{-1} and peaks at 3,448 cm^{-1} from the vibration and deformation of O–H groups [36]. The absorption peak at approximately 1,632 cm^{-1} represents the C=C stretching vibration. These structural characteristic peaks are all consistent with previous studies, indicating that SCF mainly contains carbohydrates, cellulose, lipids, alcohols, organic colloids, hydrolase, and other components. The peak positions of the main absorption peaks for the different SCF materials are similar, with slight variations in relative intensities at the same position. These results indicate that magnetized–nitrated treatment and metal loading have minimal effects on the functional group bonding structure of SCF, similar to the findings of He et al. [24]. Fig. 7b–d show the respective EDS images of SCF, MN-SCF, and $Ca(OH)_2$/Mg-MN-SCF. SCF mainly contains C, N, and O. The contents of Fe and Cl increased after magnetized–nitrated treatment. The substantial increase in Ca and Mg contents indicates the loading of Ca and Mg on the surface of $Ca(OH)_2$/Mg-MN-SCF.

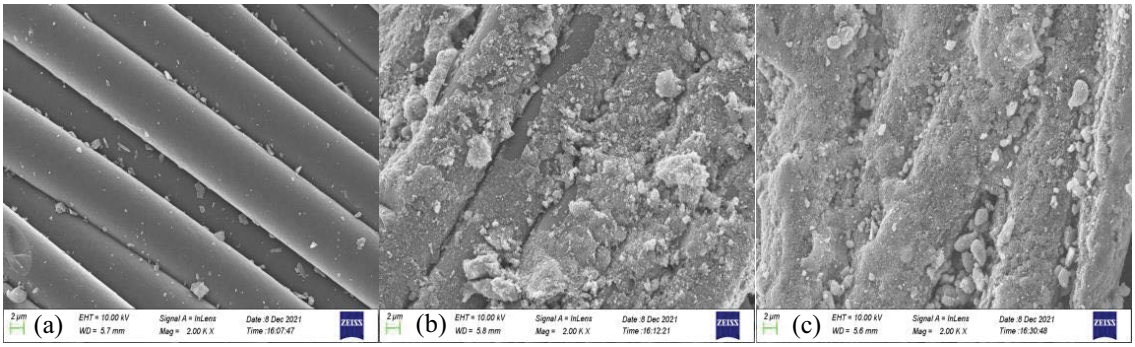

Fig. 6. SEM images of SCF (a), MN-SCF (b), and $Ca(OH)_2$/Mg-MN-SCF (c).

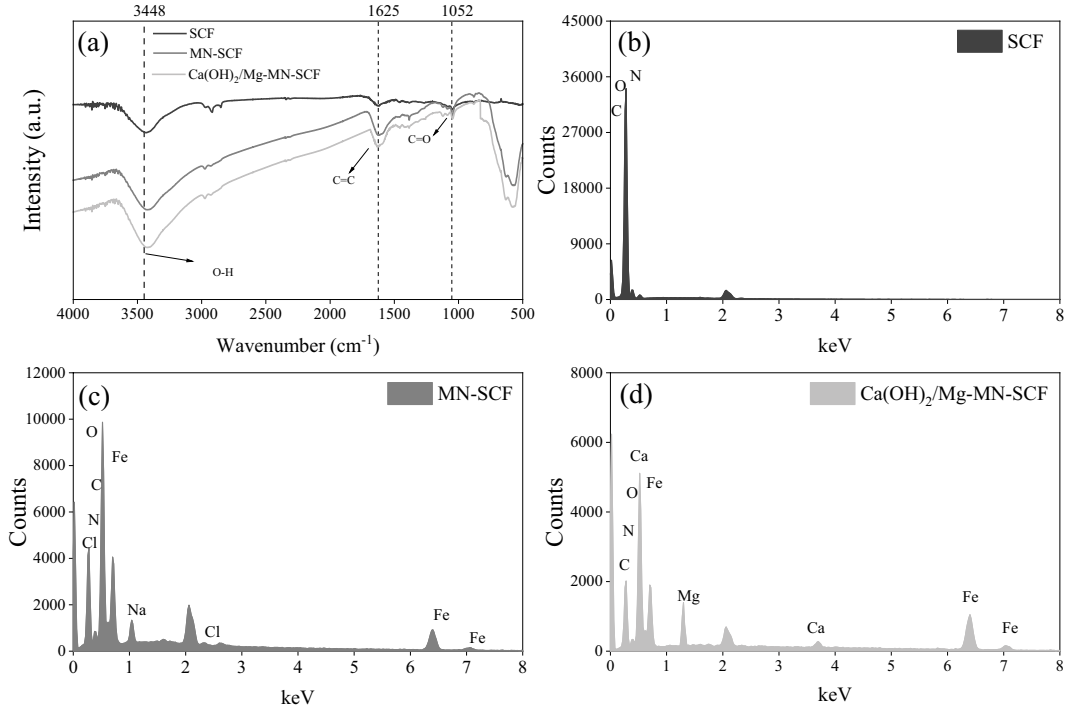

Fig. 7. FTIR (a) and EDS (b–d) characteristics of the tested SCF materials.

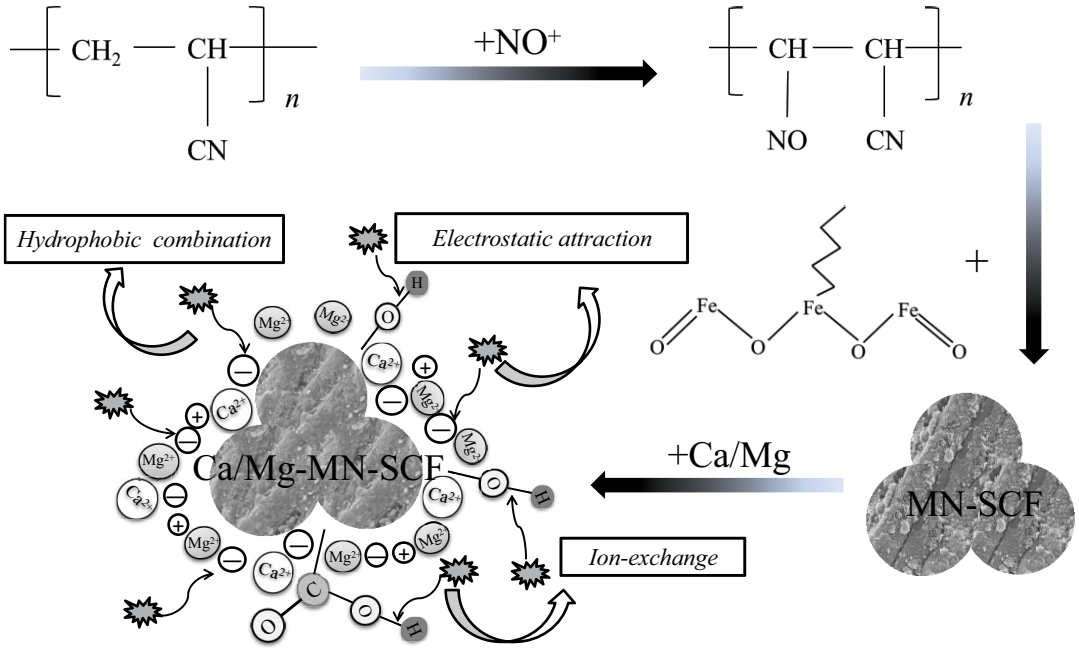

Fig. 8. Adsorption mechanism of antibiotics on different SCF materials.

3.7. Antibiotic adsorption differences among different materials

The adsorption mechanism of antibiotics on ion-loaded MN-SCF is shown in Fig. 8. The carboxyl and hydroxyl groups on the surface of SCF undergo an exchange with the functional groups in antibiotics, facilitating the adsorption of antibiotics. The adsorption mechanism occurs through electrostatic attraction, hydrophobicity, and ion exchange. The magnetized–nitrated treatment of MN-SCF increases its hydrophilicity, resulting in enhanced hydrophobic binding. The charged surface of MN-SCF can attract ions with opposite charges through electrostatic attraction [37]. Loading MN-SCF with Ca and Mg ions increases its specific surface area while reducing pore size [38]. Therefore, the surface can accommodate more positive and negative ions, strengthening ion exchange. The greater the number of ions carried on the SCF surface, the higher the adsorption capacity for pollutants.

4. Conclusion

The adsorption amounts of antibiotics on the tested materials initially increased and then decreased with increasing pH and ionic strength, reaching maximum values at pH 4 and ionic strength of 0.1 mol/L, respectively. Increasing temperature was found to enhance the adsorption of antibiotics on the tested materials. The adsorption of antibiotics by the tested materials was a chemical and monolayer adsorption process. The q_m of the three antibiotics on different materials ranged from 0.80 to 3.97 mg/g, with CTC exhibiting higher q_m compared with OTC and TC. For practical application, the materials proposed in the present study has economic, ecological and effective advantages and has high application value for antibiotic remediation. This work will provide a reference for the utilization of ion-loaded MN-SCF materials and the remediation of antibiotic-contaminated water.

Acknowledgements

The authors wish to acknowledge and thank the Sichuan Transportation Technology Project (2021-ZL-8), the Fundamental Research Funds of China West Normal University (20A022), and the Tianfu Scholar Program of Sichuan Province (2020-17).

Conflict of interests

The authors declare that they have no conflict of interest.

References

[1] P. Liu, X. Wang, L. Feng, Occurrence, resources and risk of antibiotics in aquatic environment: a review, Environ. Eng., 38 (2020) 36–42.
[2] Y. Zou, H.Y. Deng, M. Li, Y.H. Zhao, W.B. Li, Enhancing tetracycline adsorption by riverbank soils by application of biochar-based composite materials, Desal. Water Treat., 207 (2020) 332–340.
[3] N. Li, G.P. Sheng, Y.Z. Lu, R.J. Zeng, H.Q. Yu, Removal of antibiotic resistance genes from wastewater treatment plant effluent by coagulation, Water Res., 111 (2017) 204–212.
[4] Q.Q. Zhang, G.G. Ying, C.G. Pan, Y.S. Liu, J.L. Zhao, Comprehensive evaluation of antibiotics emission and fate in the river basins of China: source analysis, multimedia modeling, and linkage to bacterial resistance, Environ. Sci. Technol., 49 (2015) 6772–6782.
[5] C. Huang, S. Peng, A. Wu, H. Cai, Y. He, J. Deng, Study on the adsorption performance of sawdust biochar composite for tetracycline, Hunan. For. Sci. Technol., 48 (2021) 56–60.
[6] X. Liu, S. Lu, W. Guo, B. Xi, W. Wang, Antibiotics in the aquatic environments: a review of lakes, China, Sci. Total Environ., 627 (2018) 1195–1208.

[7] A. Almasi, Z. Rostamkhani, S.A. Mousavi, Adsorption of Reactive red 2 using activated carbon prepared from walnut shell: batch and fixed bed studies, Desal. Water Treat., 79 (2017) 356–367.
[8] S. Praveen, J. Jegan, T.B. Pushpa, R. Gokulan, L. Bulgariu, Biochar for removal of dyes in contaminated water: an overview, Biochar, 4 (2022) 10–26.
[9] B. Lian, J. Wu, K. Zhao, Z. Ye, F. Yuan, Novel insight into the adsorption mechanism of Fe-Mn oxide-microbe combined biochar for Cd(II) and As(III). Environ. Sci., 43 (2022) 1584–1595.
[10] L. Zhang, Y. Wang, J.J. Zhen, S.W. Jin, Removal of Antibiotic-Sulfadiazine From Water by Using Activated Carbon Fiber Adsorbent, CN105948158A, 2016.
[11] W. Zhao, B. Jia, Y. Zhang, J. Guan, J. Qu, Y. Lu, Study on electro-sorption of heavy metals and sulfamethoxazole on activated carbon fibers, J. Electrochem., 25 (2019) 669–681.
[12] X. Liu, L. Rao, Y. Yao, H. Chen, Phosphorus-doped carbon fibers as an efficient metal-free bifunctional catalyst for removing sulfamethoxazole and chromium(VI), Chemosphere, 246 (2020) 125783, doi: 125783.
[13] X. Li, The Preparation and Nitration Reductive Modification of Different Mesoporous Carbon for Enhanced Adsorption Mechanism of Cu(II), Nanjing Agricultural University, Nanjing, 2016.
[14] Y.J. Zhang, W.B. Li, L. Ma, L. Kang, X.L. Shi, H.Y. Deng, W. Liu, Z.F. Meng, Enhanced sorption of phenanthrene on purple soil by adding amphoteric-modified magnetized biochar, Earth Environ., 47 (2019) 745–751.
[15] L.F. Shen, J. Dong, S.D. Shan, W.J. Shu, Influence of magnetic biochar preparation methods on adsorption characteristics of Pb^{2+} in wastewater, Environ. Eng., 39 (2021) 48–55.
[16] Y. Sun, X. Yan, Y. Zhang, W. Du, J. Lu, Main modification methods of biochar and its application in pollutant removal, Contemp. Chem. Ind., 48 (2019) 1700–1703.
[17] J. Chen, W. Li, W. Ding, X. Wang, C. Hu, Removal of ammonia nitrogen by Fe/Mg-modified bamboo charcoal, China J. Environ. Eng., 9 (2015) 5187–5192.
[18] T.U. Zhu, Z.L. Lu, Y.E. Liu, C.W. Wang, K.N. Xu, Effects of preparation conditions of Mg-modified biochar on the removal of ammonium and phosphate in wastewater, Environ. Eng., 36 (2018) 37–41.
[19] Y.C. Zhi, X. Lai, B.C. Tan, X.F. Wang, Z.W. Wang, J. Li, G.L. Zhang, Adsorption of nitrate by iron, manganese and magnesium ion modified biochars, J. Nucl. Agric. Sci., 34 (2020) 1588–1597.
[20] X. Hu, S. Ma, L. Yao, C. Bai, Research progress in the removal of tetracycline antibiotics from water by modified plant biochar, Chemistry, 85 (2022) 221–227.
[21] Q. Yang, P. Wu, Preparation of modified porous biochar and its adsorption properties for tetracycline in water, Acta Sci. Circum., 39 (2019) 3973–3984.
[22] A. Abdel-Nasser, E. Hendawy, Influence of HNO_3, oxidation on the structure and adsorptive properties of corncob-based activated carbon, Carbon, 41 (2003) 713–722.
[23] Y. Fan, B. Qian, L. Wang, Y. Min, Adsorption of organic micropollutants on modified activated carbons, Environ. Chem., 20 (2001) 444–448.
[24] H. He, Preparation of Amphoteric-Magnetized Carbon-Based Clay and Its Adsorption of Tetracycline and Phenanthrene, China West Normal University, Nanchong, 2021.
[25] H.Y. Deng, H.X. He, W.B. Li, T. Abbas, Z.F. Liu, Characterization of amphoteric bentonite-loaded magnetic biochar and its adsorption properties for Cu^{2+} and tetracycline, PeerJ, 10 (2022) 13030–13049.
[26] W.B. Li, X.Y. Chen, H.Y. Deng, D. Wang, J.C. Jiang, Y.Z. Zeng, L. Kang, Z.F. Meng, Effects of exogenous biochar on soil tetracycline adsorption in Jialing River Basin, Chin. J. Soil Sci., 51 (2020) 487–495.
[27] R.A. Figueroa, A.A. Leonard, A.A. Mackay, Modeling tetracycline antibiotic sorption to clays, Environ. Sci. Technol., 38 (2004) 476–4833.
[28] L. Lin, Q. Huang, Z. Liu, Z. Song, Preparation of biochar-ferro manganese oxide composite material and properties of removal of arsenic(III)from aqueous solution, J. Agric. Resour. Environ., 34 (2017) 182–188.
[29] J.R. Pils, D.A. Laird, Sorption of tetracycline and chlortetracycline on K-and Ca-saturated soil clays, humic substances, and clay-humic complexes, Environ. Sci. Technol., 41 (2007) 1928–1933.
[30] S. Yu, H. Tang, D. Zhang, S. Wang, M. Qiu, G. Song, D. Fu, B. Hu, X. Wang, MXenes as emerging nanomaterials in water purification and environmental remediation, Sci. Total Environ., 811 (2022) 152280–152291.
[31] W. Zhang, Application of bentonite in adsorption of organic pollutants from water, Environ. Protect. Chem. Ind., 38 (2018) 267–274.
[32] X. Wang, Z. Meng, X. Liu, T. Wang, X. Hu, X. Sun, Adsorption of tetracycline and norfloxacin by BS-18 amphoteric modified bentonite, Environ. Sci., 42 (2021) 2334–2342.
[33] Y. Liu, Y. Bao, Research progress of tetracycline antibiotics contamination in soil, Environ. Pollut. Control., 8 (2011) 81–86.
[34] S. Du, Antibiotic residues in the environment, health risks and management technology review, Environ. Sci. Technol., 44 (2021) 37–48.
[35] M. Ahmed, J. Zhou, H. Ngo, W. Guo, Adsorptive removal of antibiotics from water and wastewater: progress and challenges, Sci. Total Environ., 532 (2015) 112–126.
[36] Y.F. Wang, W.B. Li, H.Y. Deng, L. Zhu, J.Q. Li, M.T. Guo, Z.F. Liu, Effect mechanism of litter extract from *Alternanthera philoxeroides* on the selective absorption of heavy metal ions by amphoteric purple soil, J. Environ. Manage., 321 (2022) 115970, doi: 10.1016/j.jenvman.2022.115970.
[37] X. Li, D. Wang, T. Zhang, Adsorption–desorption behavior of oxytetracycline (OTC) and chlortetracycline (CTC), J. Geo. Environ., 5 (2015) 317–322.
[38] L. Lin, Q. Huang, Z. Liu, Z. Song, Preparation of biochar-ferro manganese oxide composite material and properties of removal of arsenic(III) from aqueous solution, J. Agric. Resour. Environ., 34 (2017) 182–188.